



Bimetallic and trimetallic catalyzed carbon nanotubes for aqueous H₂, Cl₂ fuel cell electrodes

U.B. Suryavanshi, C.H. Bhosale*

Electrochemical Material Laboratory, Department of Physics, Shivaji University, Kolhapur (MH), India

ARTICLE INFO

Article history:

Received 25 June 2008

Received in revised form 25 August 2008

Accepted 14 September 2008

Available online 29 November 2008

Keywords:

Nanostructures
Vapour deposition
X-ray diffraction

ABSTRACT

Chemical vapour deposition (CVD) based synthesis of carbon nanotubes (CNTs) within the pores of porous ceramic substrates, using turpentine oil as a precursor, has been examined. Composites of Pt–Sn, Pt–Ni, Ni–Sn and Pt–Sn–Ni catalysts are tried for growing CNTs. In the CVD process, a reactor temperature of 1100 °C is maintained for the carbon deposition. Pt, Sn, and Ni catalysts are deposited with sputter coater, vacuum deposition and electrodeposition techniques respectively. The materials are characterized by X-ray diffraction (XRD), scanning electron microscopy (SEM), Raman spectroscopy, Fourier transform infrared spectroscopy (FTIR) and resistivity measurements by the Van der Pauw method. The prepared electrodes are tested for aqueous H₂, Cl₂ fuel cells. The Linear Sweep Voltametry (LSV) characteristics and chronoamperometry (CA) of a half cell (i.e. hydrogen electrode coated with different electrocatalysts) with 40% KCl solution are measured. Composite of Pt+Ni+Sn coated carbon nanotubes shows better performance than other tried catalysts.

© 2008 Elsevier B.V. All rights reserved.

1. Introduction

Carbon nanotubes are unique whose outstanding properties have sparked an abundance of research since their discovery in 1991 [1]. These nanomaterials are very promising for the development of novel, technological applications such as batteries [2], tips for scanning probe microscopy [3], electrochemical actuators [4], sensors [5] etc. In addition to initially developed laser furnace [6] and arc discharge [7] techniques, catalytic chemical vapour deposition (CCVD) method [8–11] has been contrived for a scalable, large scale production of carbon nanotubes, with various carbon source molecules tested such as carbon monoxide, methane, benzene, xylene, toluene etc. These carbon sources are related to fossil fuels which may not be sufficient in near future; so researchers from IIT Bombay switched over to reproducible natural carbon source: camphor and grown various kind of nano-carbons [12–15]. Kumar and Ando reported condition of growing multi-walled carbon nanotubes (MWNTs) [16,17] single-walled carbon nanotubes (SWNTs) [18] and vertically aligned carbon nanotubes [19] with well-valued material camphor [20]. This gives new idea to develop nanotechnology with ecofriendly carbon source: turpentine oil, which is derived from the oleoresin of *Pinus* species particularly from *Pinus Palus-*

tris of pinaceae family. A simple template synthesis method has been explored [21–24] for preparing micro- and nanostructured materials. This method entails synthesizing the desired material within the pores of porous ceramic membrane and has been used to make tubules and fibrils composed of polymers, metals [25], semiconductors [26], metal oxides [27], carbon [28] and composite materials [5,29]. Primary interest is in the production of carbon nanotubes that could be used as anode in aqueous H₂, Cl₂ fuel cells. In caustic soda industries chlorine releases as byproduct and purpose is to utilize it electrochemically and produce power as well as HCl. Initial cost of fuel cell due to platinum electrodes is the main challenge in commercialization of fuel cells. CNT may solve this problem as it has high conductivity and porosity for gas diffusion. This approach includes CVD based synthesis of carbon thin film within the pores of ceramic membrane with catalyst deposited in the pores. In the present work, different catalysts like Pt–Sn, Pt–Ni, Ni–Sn and Pt–Sn–Ni have been deposited with electrodeposition, sputter coating and vacuum deposition techniques. The formed electrodes have been further used for structural and electrical characterization.

2. Experimental

2.1. Carbon deposition

Porous ceramic were cut into small size of 2 cm × 2 cm × 0.2 cm and were used as a substrate for growing carbon nanotubes using CVD method. The CVD unit consisted of two furnaces joined side by side with a quartz tube traversing horizontally along the axis of both of them. The vapourizing furnace (A) was used to

* Corresponding author. Tel.: +91 231 2609228; fax: +91 231 2691533.
E-mail addresses: ubsuryavanshi@yahoo.com (U.B. Suryavanshi),
chb.phy@unishivaji.ac.in (C.H. Bhosale).

vapourise turpentine oil ($C_{10}H_{16}$) and that of pyrolysing furnace (B) was used to pyrolyse the turpentine oil vapours. Nitrogen gas was flushed at the flow rate 160 ml/min through the tube for 15 min before starting the deposition to remove the air completely. A quartz boat containing 3 ml of turpentine oil was placed in the furnace A, maintained at optimized temperature i.e. at 250 °C with temperature controller (Aplab make, Model No. 9601). The temperature of furnace (B) containing ceramic substrates was maintained at optimized 1100 °C with the help of temperature controller (SELEC make, Model No. DTC324). At this temperature, conducting carbon was deposited which is the basic need of fuel cell electrodes. The deposition was carried out for 1 h under the nitrogen flow. Nitrogen gas flushed until the furnaces were cooled down to room temperature and then samples were collected.

2.2. Electrodeposition of nickel

Catalyst loading is the important part in growing carbon nanotubes. Nickel films were deposited onto carbon coated ceramic from an electrolytic bath containing 1N concentration of $Ni(NO_3)_2 \cdot 6H_2O$ for 30 min. Films were deposited at a potential of 0.55 V with respect to saturated calomel electrode (SCE), the reference electrode. Electrodeposition was carried out on the 2 cm × 2 cm area of the substrates at potentiostatic mode in an unstirred bath at room temperature. After deposition, the films were rinsed in double distilled water and were used for further deposition of carbon.

2.3. Deposition of platinum

Pt was deposited with JEOL JFC-1600 auto fine magnetron type sputter coater consisting of a basic unit (350 mm wide × 340 mm deep × 282 mm high, 12 kg) and rotary pump unit (280 mm wide × 120 mm deep × 215 mm high, 10 kg). Standard Pt of 57 mm in diameter was used as a target. The specimen stage size was adjusted at the height of 35 mm and pressure at 10^{-1} Pa. Coating time was set for 30 s and sputtering current was about 40 mA. The films have been deposited with 15 nm thickness.

2.4. Deposition of tin

Sn was deposited with 'HINDHIVAC vacuum coater model - 12A4D consisting of vacuum chamber and pumping system. The chamber is evacuated by HINDHIVAC diffpack pump model-114D and backed by 200 l/min, double stage, direct driven, rotary pump, model ED-12 with an overload protection. The films of Sn were vacuum deposited by Sn foil (99% pure, Merck) with resistive heating using molybdenum boat. The deposition was carried out on porous ceramic substrates under vacuum more than 10^{-5} mbar. The thickness and deposition rates were monitored with quartz crystal monitor (DTM 101 operated at 6 MHz). The films with 15 nm thickness were deposited at deposition rate 10 Å/s.

Different combinations of catalysts like Pt-Sn, Pt-Ni, Ni-Sn and Pt-Sn-Ni have been tried for growing carbon nanotubes.

2.5. Growing of carbon nanotubes

Carbon nanotubes were grown onto the catalyst coated carbon thin films by CVD with turpentine oil (3 ml) as a precursor kept at 250 °C and pyrolysed at 1100 °C.

2.6. Characterization of grown carbon nanotubes

Structural properties of prepared carbon electrodes were studied by XRD technique. XRD studies were carried out with Phillips analytical PW 1710 X-ray diffractometer. X-ray machine was operated at 40 kV, 30 mA, using $Cu K\alpha_1$ and $K\alpha_2$ radiation having wavelengths $\lambda = 1.54056$ and 1.54439 \AA respectively. The XRD patterns for these materials were recorded within the span of angles between 10° and 100° for nickel catalyzed carbon films. Micro-structure investigation has been studied with SEM (JEOL JSM 6360, Japan). For this purpose platinum (15 nm) was coated by Polaron sputter coater unit E-2500. Raman spectra of these samples were taken with cofocal Raman microscope (CRM 200, WiTec, USA). Raman spectra of as grown CNTs were measured by green laser with wavelength of 532 nm and power of 14.4 mW. Each spectrum was performed with 30 s acquisition time, an illumination spot size of 1 μm . FTIR spectra were recorded on a Perkin-Elmer spectrum-1 spectrophotometer. The samples were made according to the technique of Stimson and Schiedt. Sample powder is mixed with KBr and a homogeneous mixture is formed with a mortar and pestle. This mixture was placed in a cylindrical dye of 13 mm diameter and pressed for about 5 min at 200 kg/cm² to make pellet. These pellets were then kept in a dry box for 10 min. Then these pellets were scanned in the frequency range of 450–4000 cm^{-1} . FTIR patterns of the porous ceramic were subtracted from the FTIR pattern of samples with a carbon deposit to get the actual pattern of deposited carbon. Resistivity of the samples was measured with Van der Pauw technique.

2.7. Half cell performance

The electrochemical performance of the hydrogen electrode was studied with half cell configuration. Half cell tests were carried out in conventional three

electrode cell consisting of the electrode to be tested (working electrode), a platinum foil of dimensions 2 cm × 2 cm × 0.1 cm (counter electrode) and saturated calomel electrode (SCE) as a reference electrode. 40% KCl solution was used as electrolyte at room temperature. The actual cell configuration was 'hydrogen electrode, $H_2/40\% KCl (SCE)/Pt$ '. All electrochemical measurements were performed with potentiostat, EG and G make VersaStat - II model, controlled by electrochemistry software M270. The same flow rate of hydrogen was maintained in all experiments.

2.7.1. Linear Sweep Voltametry (LSV)

LSV was employed to study the reduction of hydrogen with respect to catalyst activated carbon nanomaterials. The potential of working electrode was scanned from initial potential to final potential (−500 to +700 mV vs SCE) with scan rate (20 mV/s) as a ramp.

2.7.2. Chronoamperometry (CA)

In chronoamperometry, the time dependent deposition current density $I(t)$ is recorded for measuring half cell performance of hydrogen on particular working electrode at constant. The CA was measured at reduction potential for each electrode calculated with LSV and by applying potential step of 0.2 V. The performance was firstly measured for 10 s only and the electrodes, which were giving noticeable performance, measured for 3600 s. $I-t$ characteristics was studied for the

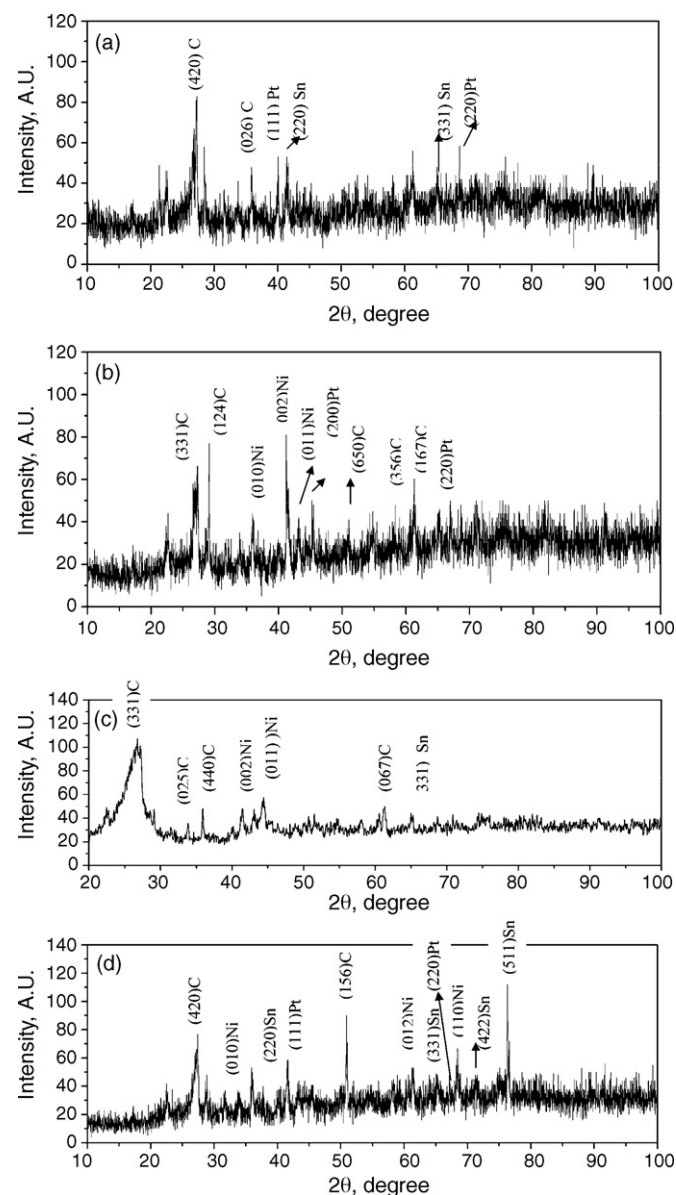


Fig. 1. XRD patterns of the carbon nanotubes catalyzed with (a) Pt-Sn; (b) Pt-Ni; (c) Ni-Sn; (d) Pt-Sn-Ni.

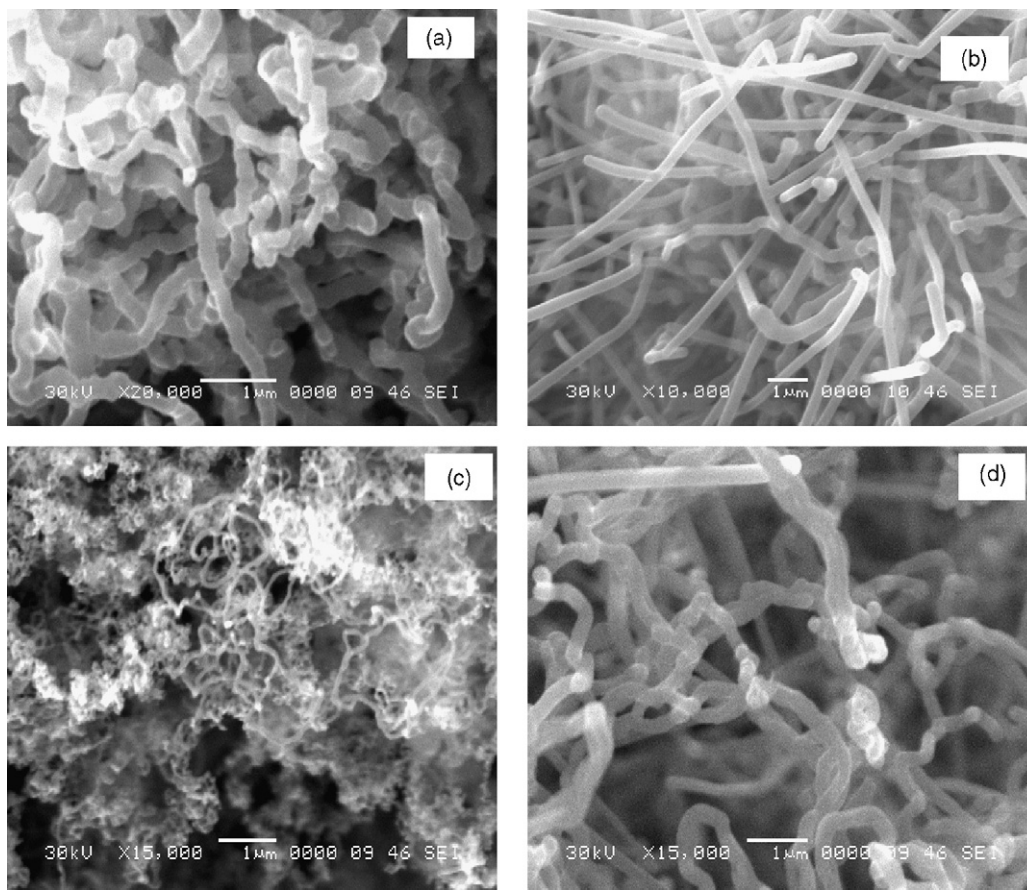


Fig. 2. SEM images of the carbon nanotubes catalyzed with (a) Pt-Sn; (b) Pt-Ni; (c) Ni-Sn; (d) Pt-Sn-Ni.

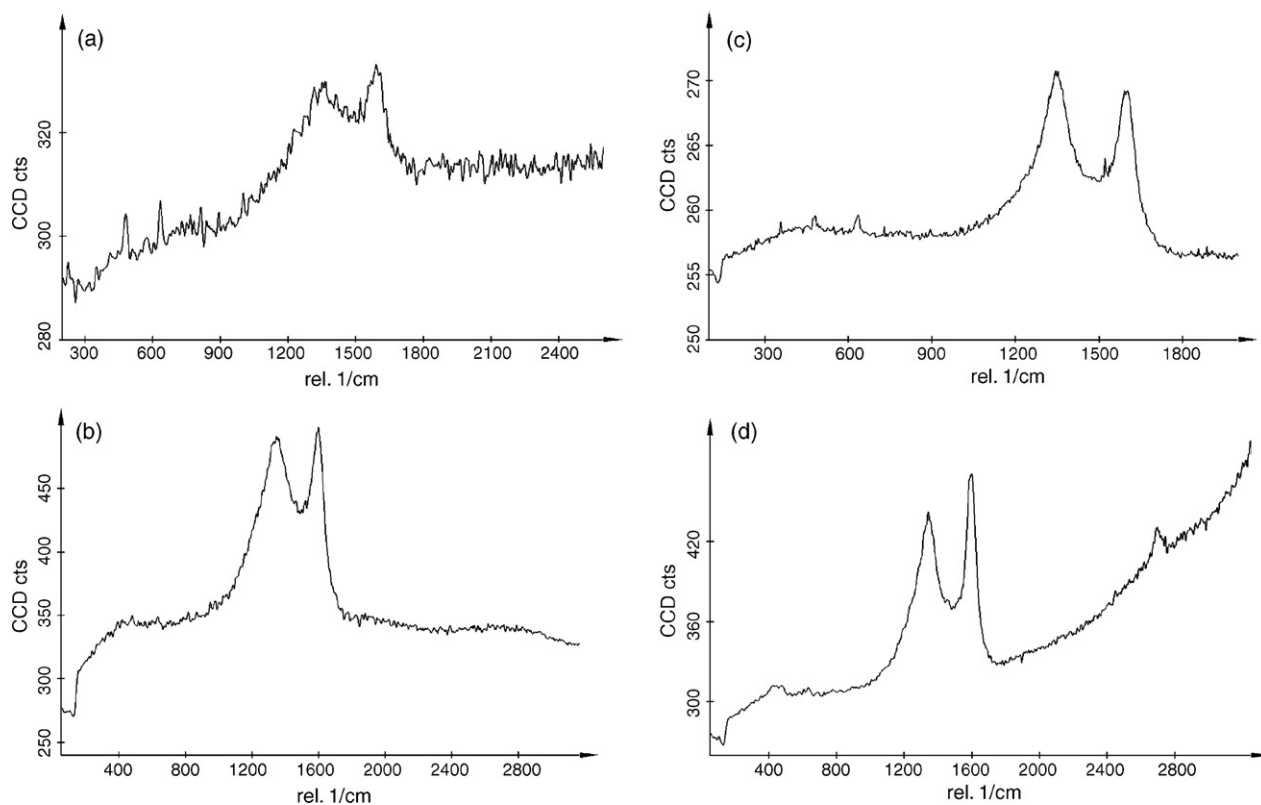


Fig. 3. Raman spectra of the carbon nanotubes catalyzed with (a) Pt-Sn; (b) Pt-Ni; (c) Ni-Sn; (d) Pt-Sn-Ni.

electrodes which give remarkable performance while scanning chronoamperometry.

3. Results and discussion

When a volatile compound of the substance to be deposited is vapourized and the vapour is thermally decomposed or reacted with other gases, vapours or liquids at the substrate to yield non-volatile reaction products which deposit atomistically (atom by atom) on the substrate, the process is called chemical vapour deposition [30,31].

3.1. X-ray diffraction studies

Fig. 1(a)–(d) shows the XRD patterns for Pt–Sn, Pt–Ni, Ni–Sn and Pt–Sn–Ni catalyzed carbon nanotubes. All the XRD patterns show microcrystalline nature of the films with characteristic graphite peaks. Conducting carbon i.e. graphitic carbon is the basic need for the fuel cell electrodes which gets fulfilled in these prepared electrodes.

3.2. Scanning electron microscopy studies

Fig. 2(a)–(d) shows SEM micrographs for Pt–Sn, Pt–Ni, Ni–Sn and Pt–Sn–Ni catalyzed carbon thin films deposited on porous ceramic. All micrographs show well-grown carbon nanotubes. In SEM image of Pt–Sn catalyzed carbon nanotubes (Fig. 2(a)) coiled structure of carbon nanotubes have been observed. The average diameter of these carbon nanotubes is nearly 200 nm. Pt–Ni catalyzed carbon nanotubes (Fig. 2(b)) show randomly oriented carbon nanotubes of diameter nearly 100 nm only. Ni–Sn catalyzed carbon nanotubes (Fig. 2(c)) show blurred image of formed carbon nanotubes having diameter less than that of 100 nm. Pt–Sn–Ni catalyzed carbon nanotubes (Fig. 2(d)) show coiled structure of carbon nanotubes of diameter 200–300 nm. So each tried catalyst enhances the growth of carbon nanotubes while Pt–Ni and Ni–Sn catalyzed carbon nanotubes are of low diameter (~100 nm). In both case nickel is the common catalyst, which may catalyze the reaction in such a way that the formed carbon nanotubes are of lower diameter than that of other catalyst.

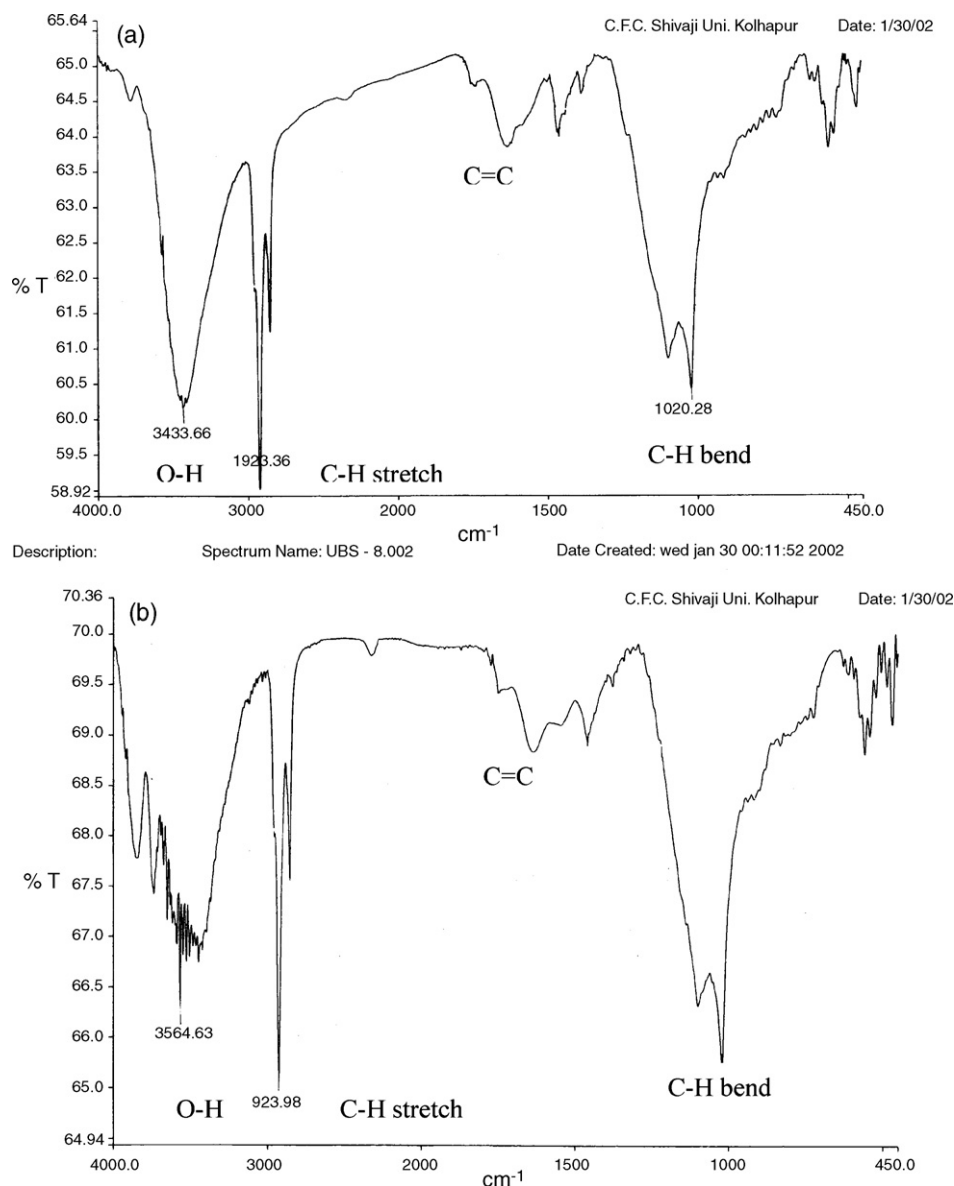


Fig. 4. FTIR patterns of the carbon nanotubes catalyzed with (a) Pt–Sn; (b) Pt–Ni; (c) Ni–Sn; (d) Pt–Sn–Ni.

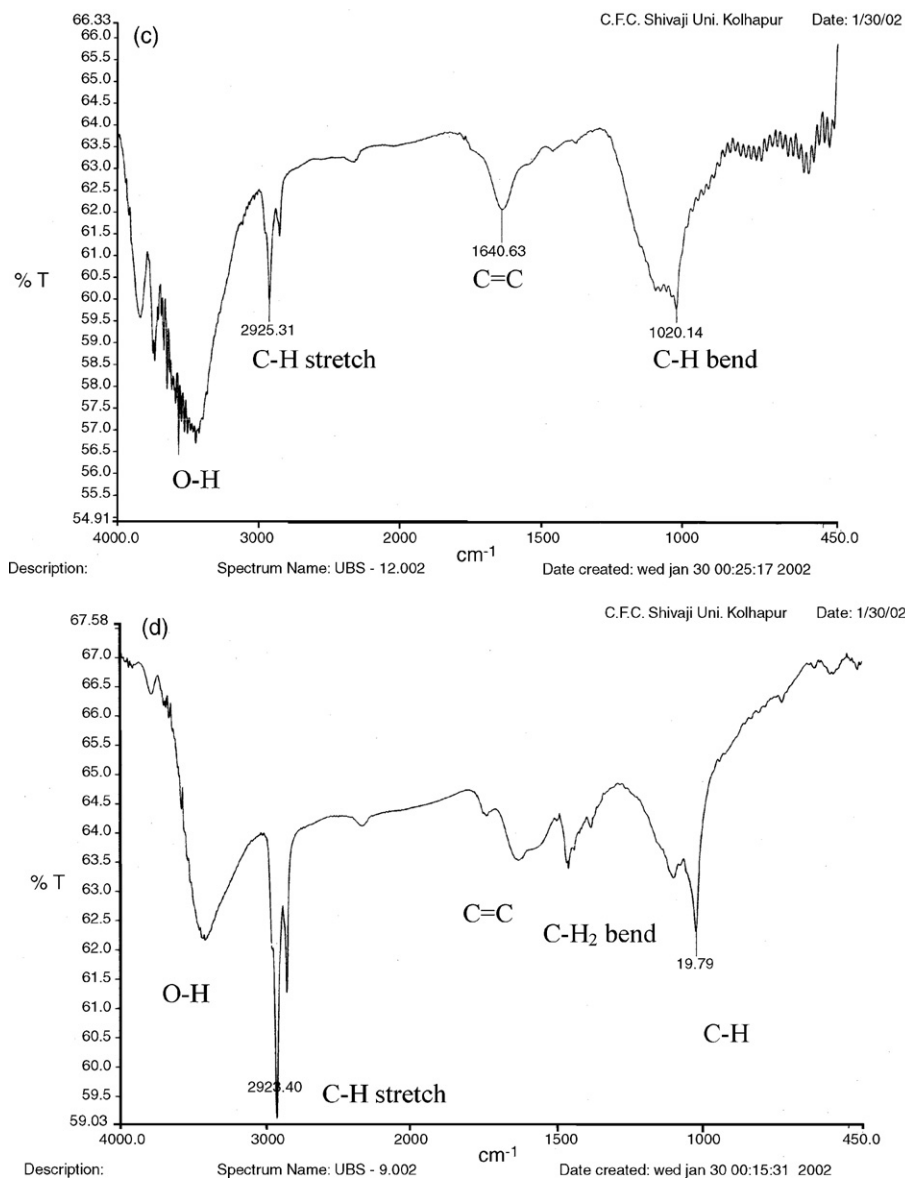


Fig. 4. (Continued).

3.3. Raman spectroscopy studies

Raman spectroscopy is a sensitive method for CNT characterization. Due to specific combination of strong Van Hove singularities of the phonon density and Raman resonance effect it is possible to measure Raman scattering spectra of small bundles or even of single nanotube. Fig. 3(a), (b), (c) and (d) shows the Raman spectra of the films catalyzed with Pt–Sn, Pt–Ni, Ni–Sn and Pt–Sn–Ni respectively. The well-separated two peaks (G and D) are clearly observed for all samples. G-peak (around 1600 cm^{-1}) corresponds to tangential stretching mode (E_{2g}) of highly oriented pyrolytic graphite and suggests CNTs are composed of crystalline graphitic carbon and D-peak (around 1300 cm^{-1}) originates from disorder in the sp^2 hybridized carbon and indicates lattice distortion in the curved graphene sheets, tube ends etc. [32]. From Fig. 3 it is observed that G-peak intensity is maximum for Pt + Ni + Sn catalyzed CNTs while for Ni + Sn catalyzed CNTs D-peak intensity is more than that of G-peak intensity. This is because of defects in the tube such as pentagons, curvature etc. The lower frequency Radial Breathing Mode (RBM) peaks are observed for Pt + Sn catalyzed CNTs but its inten-

sity is too low. This indicates the formation of single-walled CNTs but it might be of less in number.

3.4. Fourier transform infrared spectroscopy

To study the nature of carbon nanotubes, FTIR were taken. Fig. 4(a), (b), (c) and (d) shows the FTIR spectrum of the films catalyzed with Pt–Sn, Pt–Ni, Ni–Sn and Pt–Sn–Ni respectively. All three graphs show three major peaks of O–H, C–H stretch and C=C. The peak of $1019\text{--}1020\text{ cm}^{-1}$ is a substrate peak. C=C shows the graphitic nature of the carbon nanotubes. Both graphs shows two major peaks in the range of $2850\text{--}2920\text{ cm}^{-1}$ corresponding to sp^3 and sp^2 carbon atoms respectively, because it has been reported that the absorption for C–H stretching vibrations on sp^2 bonded carbons is found in the range $2920\text{--}3060\text{ cm}^{-1}$ while for sp^3 carbons in the range $2850\text{--}2915\text{ cm}^{-1}$ [13]. From FTIR, calculated ratio of sp^2 to sp^3 is nearly equal to 2 for Pt + Sn catalyzed CNTs and it is greater than 2 for other tried catalysts. The percentage of sp^2 carbon atoms is around 86% for Pt + Sn and for others nearly 90% indicating more graphite in the deposited material. This calculation suggests

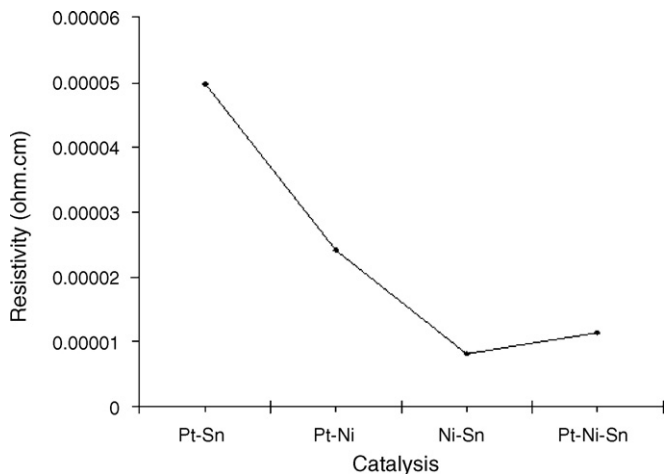


Fig. 5. Resistivity measurement by Van der Pauw technique for carbon nanotubes catalyzed with Pt-Sn, Pt-Ni, Ni-Sn and Pt-Sn-Ni.

that presence of relatively small percentage of sp^2 carbon atoms in deposited CNTs. From results it can be observed that turpentine oil having formula $C_{10}H_{16}$ decomposes at 1100°C and forms carbon nanotubes which are graphitic in nature.

3.5. Resistivity by Van der Pauw technique

Fig. 5 shows the resistivity of carbon nanotubes catalyzed with Pt-Sn, Pt-Ni, Ni-Sn and Pt-Sn-Ni. All carbon films show low resistivity (in the range of $10^{-6}\ \Omega\text{cm}$) where the CNT catalyzed with

Ni-Sn show lowest resistivity i.e. $8.083 \times 10^{-6}\ \Omega\text{cm}$. That means formed carbon nanotubes are highly conducting i.e. of graphitic nature. The same conclusion has been drawn from X-ray diffraction pattern.

3.6. Half cell performance

When hydrogen gas passes through catalyst activated carbon nanomaterials, which are coated on porous ceramic substrates, hydrogen dissociates into hydrogen ions and electrons. The ions pass through 40% KCl solution while that of electrons through outer circuit. When two phases are brought together to form a boundary, differences of chemical and electrochemical potential cause mobile charge carriers i.e. ions, to migrate until free energy equilibrium is reached and a separation of charge results. The force of electrostatic attraction limits the distances to which the charges can be separated; resulting double layer formation. The charges in the two layers are equal and opposite. At such boundaries, tendency of ions to move across such double layers contribute importantly to E , the driving force of the overall cell reaction [19].

3.6.1. Linear Sweep Voltametry

Fig. 6(a), (b), (c) and (d) shows LSV for the CNTs catalyzed with Pt-Sn, Pt-Ni, Ni-Sn and Pt-Sn-Ni respectively. Fig. 6(a) shows the I region in which appreciable potential drop occurs due to electrode-electrolyte interface resulting from the bending of bands. The starting value of the I region current density is $-375\ \mu\text{A}/\text{cm}^2$. When scanning potential enters in the region II, the current curve is becoming flat due to equilibrium anodic and cathodic current. In region III, cathodic current starts to increase. It represents the starting of reduction of hydrogen and further

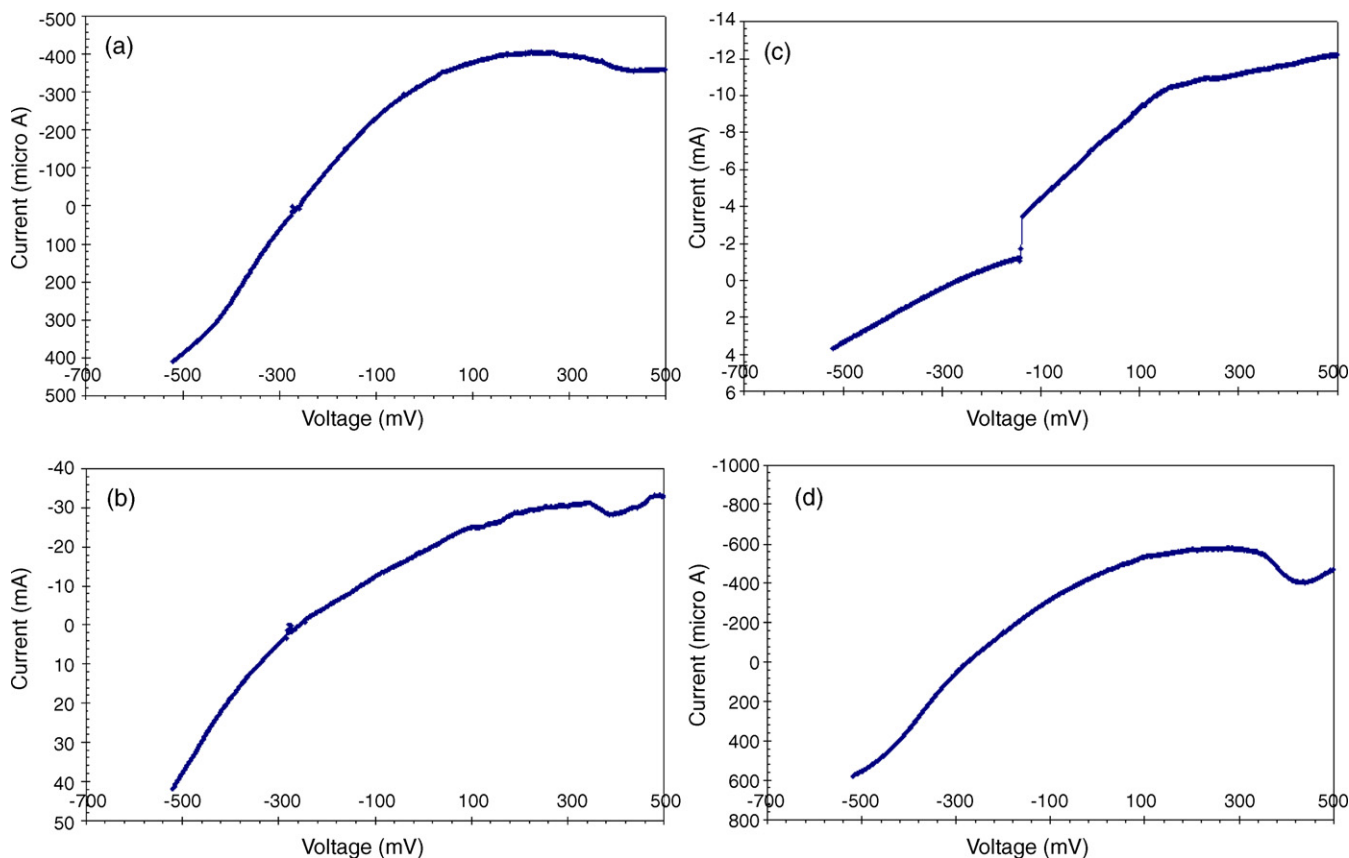


Fig. 6. Linear Sweep Voltametry (LSV) of the carbon nanotubes catalyzed with (a) Pt-Sn; (b) Pt-Ni; (c) Ni-Sn; (d) Pt-Sn-Ni.

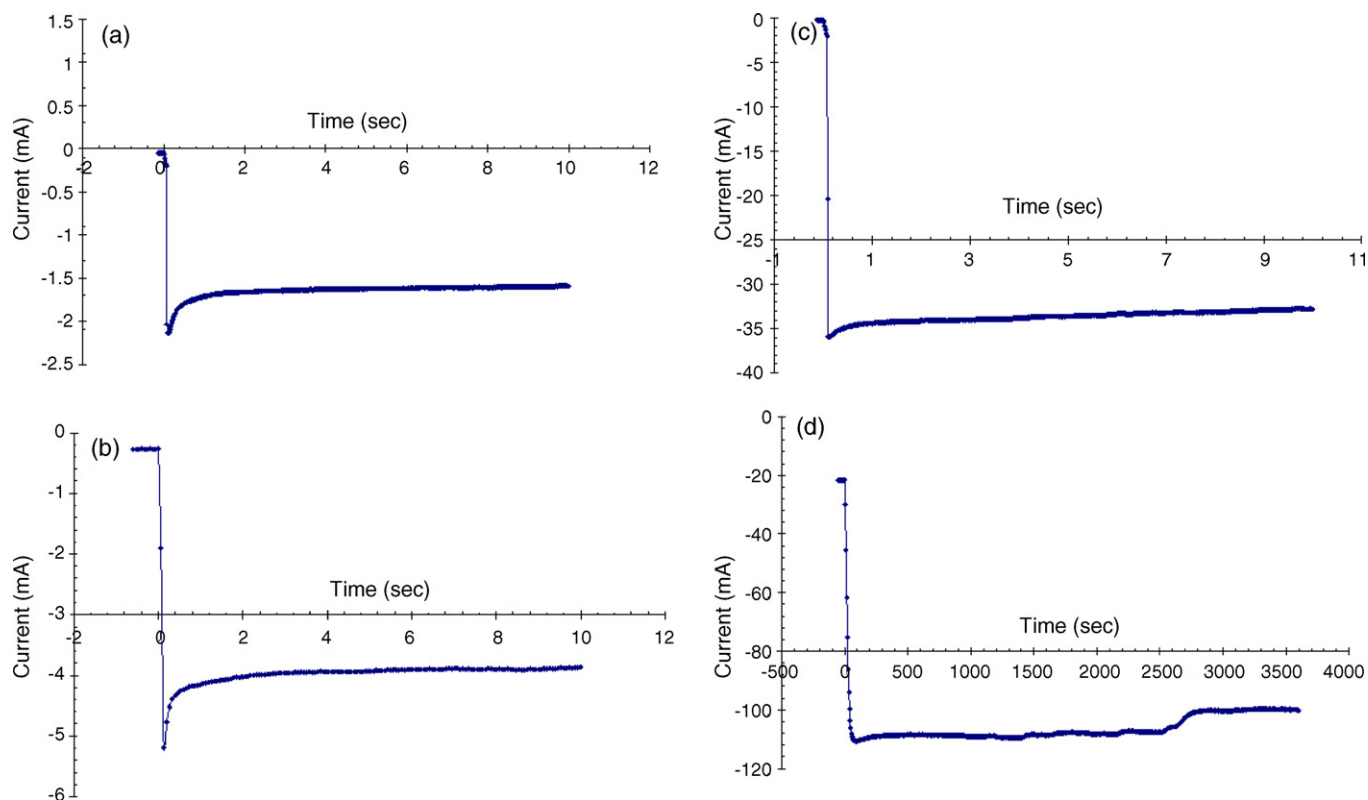


Fig. 7. Chronoamperometry of the carbon nanotubes catalyzed with (a) Pt–Sn; (b) Pt–Ni; (c) Ni–Sn; (d) Pt–Sn–Ni.

sharp increase in current up to $400 \mu\text{A}/\text{cm}^2$. Fig. 6(b) shows the reduction potential of hydrogen on Ni + Pt in positive region with respect to SCE. While hydrogen reduces on Ni + Sn and Pt + Sn + Ni catalyzed CNTs at -140 and -75 mV respectively with respect to SCE [Fig. 6(c) and (d)]. That means Pt + Sn + Ni catalyzed CNTs dissociates hydrogen at low potential.

3.6.2. Chronoamperometry

In a chronoamperometry, fuel cell performance shows variation of current density with respect to time at constant potential i.e. at reduction potential of hydrogen. Fig. 7(a), (b), (c) and (d) shows CA curve CNTs catalyzed with Pt–Sn, Pt–Ni, Ni–Sn and Pt–Sn–Ni respectively. Fig. 7(a) and (b) shows very less current density (1.5 and $4 \text{ mA}/\text{cm}^2$ respectively) may be because of less catalytic activity for hydrogen or may be imperfect cell geometry with respect to the catalyst cone. A delicate balance must be maintained among the electrode, electrolyte and gaseous phases in the porous electrode structure. Fig. 7(c) shows CA curve for Ni + Sn catalyzed CNTs. It show first shoot within 2–5 s on $36 \text{ mA}/\text{cm}^2$ and then become stable on $34 \text{ mA}/\text{cm}^2$ current density. For combination of catalyst platinum + tin + nickel first shoot is at $115 \text{ mA}/\text{cm}^2$ and becomes stable at $110 \text{ mA}/\text{cm}^2$. As it is good performance it has been checked for 3600-s time period. But after 2500 s some degradation in performance is seen and it becomes stable at $100 \text{ mA}/\text{cm}^2$ (Fig. 7(d)).

4. Conclusions

Bimetallic and trimetallic catalyst coated CNTs on a porous ceramic are promising options for fuel cell electrodes. The ceramic substrate provides strength to the electrode as well as porosity for good diffusion of the fuel/oxidant. Simple and economical CVD method for preparing graphitic carbon nanotubes with Pt–Sn, Pt–Ni, Ni–Sn and Pt–Sn–Ni onto the pores of ceramic has been

explored. XRD, SEM, Raman spectroscopy, FTIR and resistivity measurements confirms the deposition of graphitic CNTs of low resistivity (10^{-6}) which is essential for fuel cell electrode. From LSV and CA curves, Pt + Ni + Sn coated CNTs yield high current densities. This means Pt + Ni + Sn coated CNTs can replace pure platinum electrode and reduce initial cost of fuel cell.

References

- [1] S. Iijima, Nature 354 (1991) 56–58.
- [2] T.W. Odom, J.L. Huang, P. Kim, C.M. Lieber, J. Phys. Chem. B 104 (2000) 2794.
- [3] G. Che, B.B. Lakshmi, E.R. Fisher, C.R. Martin, Nature 393 (1998) 347.
- [4] S. Wong, J.D. Harper, P.T. Lansbury, C.M. Lieber, J. Am. Chem. Soc. 120 (1998) 603.
- [5] J. Kong, R.N. Franklin, C. Zhou, M.G. Chapline, S. Peng, K. Cho, H. Dai, Science 287 (2000) 6226.
- [6] A. Thess, R. Lee, P. Nikolaev, H. Dai, P. Petit, J. Robert, C. Xu, Y.H. Lee, S.G. Kim, A.G. Rinzler, D.T. Colbert, G.E. Scuseria, D. Tománek, J.E. Fischer, R.E. Smalley, Science 273 (1996) 483.
- [7] C. Journet, W.K. Maser, P. Bernier, A. Loiseau, M.L. de la Chapelle, S. Lefrant, P. Deniard, R. Lee, J.E. Fisher, Nature 388 (1997) 756.
- [8] H. Dai, A.G. Rinzler, P. Nikolaev, A. Thess, D.T. Colbert, R.E. Smalley, Chem. Phys. Lett. 260 (1996) 471.
- [9] A.M. Cassell, J.A. Raymakers, J. Kong, H. Dai, J. Phys. Chem. B 103 (1999) 6484.
- [10] S. Maruyama, R. Kojima, Y. Miyauchi, S. Chiashi, M. Kohno, Chem. Phys. Lett. 360 (2002) 229.
- [11] M.J. Bronikowski, P.A. Willis, D.T. Colbert, K.A. Smith, R.E. Smalley, J. Vac. Sci. Technol. A 19 (2001) 1800.
- [12] K. Mukhopadhyay, K.M. Krishna, M. Sharon, Phys. Rev. Lett. 72 (1994) 3184.
- [13] K. Mukhopadhyay, M. Sharon, Mater. Chem. Phys. 49 (1997) 105.
- [14] K. Mukhopadhyay, K.M. Krishna, M. Sharon, Mater. Chem. Phys. 49 (1997) 252.
- [15] M. Sharon, K. Mukhopadhyay, K. Yase, S. Iijima, Y. Ando, X. Zhao, Carbon 56 (1998) 284.
- [16] M. Kumar, X. Zhao, Y. Ando, M. Sharon, K. Hirahara, S. Iijima, Mol. Cryst. Liq. Cryst. 387 (2002) 117.
- [17] M. Kumar, Y. Ando, Diam. Relat. Mater. 12 (2003) 998.
- [18] M. Kumar, Y. Ando, Diam. Relat. Mater. 12 (2003) 1845.
- [19] M. Kumar, Y. Ando, Chem. Phys. Lett. 374 (2003) 521.
- [20] M. Kumar, T. Okazaki, M. Hiramatsu, Ando Carbon 45 (2007) 1899.
- [21] C.R. Martin, Science 266 (1994) 1961.
- [22] C.R. Martin, Acc. Chem. Res. 28 (1995) 61.

- [23] C.R. Martin, *Chem. Mater.* 8 (1996) 1739.
- [24] G. Che, K.B. Jirage, E.R. Fisher, C.R. Martin, H. Yoneyama, J. *Electrochem. Soc.* 144 (1997) 4296.
- [25] C.R. Martin, *Adv. Mater.* 3 (1991) 457.
- [26] J.D. Klein, R.D. Herrick, D. Palmer, M.J. Sailor, C.J. Brumlik, C.R. Martin, *Chem. Mater.* 5 (1993) 902.
- [27] B.B. Lakshmi, P.K. Dorhout, C.R. Martin, *Chem. Mater.* 9 (1997) 857.
- [28] R.V. Parthasarathy, C.R. Martin, *Adv. Mater.* 7 (1995) 896.
- [29] V.M. Cepak, J.C. Hulteen, et al., *Chem. Mater.* 9 (1997) 1065.
- [30] H. Schafer, *Chemical Transport Reactions*, Academic Press Inc., New York, 1964.
- [31] C.F. Powell, J.H. Oxley, J.M. Blocher Jr. (Eds.), *Vapor Deposition*, John Wiley and Sons Inc., New York, 1996.
- [32] M.S. Dresselhaus, G. Dresselhaus, A. Jorio, A.G. Souza Filho, R. Saito, *Carbon* 40 (2002) 2043.